Design of Dynamic Airvents and Airflow Analysis in a Passenger Car Cabin

Varad M. Limaye[1], Deshpande M. D.[2], Sivapragasam M.[3], Vivek Kumar[4]

1-M.Sc. [Engg.] Student, 2-Professor, 3- Asst. Professor,
Department of Automotive and Aeronautical Engineering, M.S.Ramaiah School of Advanced Studies, Bangalore 560058
4- Manager(CFD), Tata Motors Ltd. Pune.

Abstract

Air conditioning has become a standard option on most vehicles enhancing comfort and safety. Modern systems feature automatic climate control, integrated cooling, heating, de-misting and de-frosting, air filtering, and humidity control. These systems improve passenger thermal comfort and safety.

Passenger thermal comfort is mainly influenced by the inside cabin temperature. Cabin temperature in turn depends on the cabin size, number and shape of airvents and mass flow rate of the total HVAC system, and the interior materials of dashboard, trims and seatings. Normally airvents in passenger car have manual adjustment of the vanes to set the airflow direction. An attempt has been made to make these airvents operate automatically as per the cabin temperature. The concept named dynamic airvents has been suggested in a passenger hatch and assessed by CFD analysis using commercial code FLUENT (ANSYS 13). The simulation done for all the airvents has been validated with the experimental test results. With the help of CFD simulations it is shown that dynamic airvents provide a better thermal comfort for passengers. Airflow pattern has been studied and compared with the steady airvent model. Airflow for 1 and 2 cycles of the vane movement has been simulated. The movement of the vanes is given for central vertical, horizontal vanes and side horizontal vanes. The airflow velocity due to the dynamic nature of the vanes has enhanced towards the rear passenger. Cabin cool down analysis with the dynamic vents has been done to study the effect of cooling inside the cabin. Comparison with the baseline airvents has shown that cabin cool down is achieved faster with dynamic vents. With dynamic airvents an average cabin temperature drop by almost 3°C is achieved within 25 minutes compared to the baseline. The airflow velocity, directivity and temperature drop rate with dynamic airvents is observed to be better than in the case of steady airvents.

Key Words: Computation Fluid Dynamics, Dynamic Airvents, HVAC, Car Cabin.

Abbreviations

ACC	Automatic Climate Control
CFD	Computational Fluid Dynamics
CMH	Cubic Meter per Hour
HVAC	Heat Ventilation and Air Conditioning
UDF	User Defined Functions

1. INTRODUCTION

Human comfort in cars is of prime importance nowadays, in which thermal comfort plays an important role. With the rapid development of technology and increasing demands by customers, the climate control of the passenger cabin has to be taken into account in any vehicle development process. To enhance the competitive ability of an automobile the satisfaction of customer's requirement for automotive thermal comfort is of crucial importance. However, the comfort level being subjective it is hard to set definitive levels. The only controlling measures are airflow velocity, cabin temperature and relative humidity. Hence continuous research and investigation is being done to achieve more and more thermal comfort to the passengers.

Improving air conditioning performance and occupant thermal comfort requires an understanding of the fluid motion prevailing in the cabin for required ventilation setting and passenger loading. HVAC system being the heart of air conditioning it should be properly designed and packaged for a particular car. The size of the air-conditioning system is related to the peak thermal load in the vehicle. The peak thermal load is generally related to the maximum temperature the cabin will reach while soaking in the sun. The thermal load can be further reduced by using more efficient distribution of the treated air as well as using more efficient equipment (such as by using waste heat to provide cooling). A variety of technologies to reduce climate control loads such as advanced glazing, heated/cooled seats, parked car ventilation, recirculation strategies, and air cleaning have been developed. Companies like BMW and Audi have been experimenting and using innovative techniques to cool/heat the passenger compartment for maximum thermal comfort. Features like automatic climate control, automatic air re-circulation and solar powered pre-cooling ventilation system on roof, remote-activated air-conditioning for pre-cooling the cabin, heated leather seats are now added to some vehicles. Computational fluid dynamics procedures have been applied in various studies on important components of HVAC. The passenger cabin being equipped with a lot of parts (dashboard, steering, centre console, seats etc.) the actual flow is highly non-uniform. A very fast transient behaviour during soak and cool down are observed. To capture flow parameters during the transient period involves specialised expensive equipment. Hence computational methods are now popular for preliminary test which drastically reduce development time and cost.

Lot of research was carried out to improve the thermal comfort inside the passenger car. Ruzic [1] suggested improvement of thermal comfort in a passenger car by localized air distribution. The paper provides an overview of local microclimate parameters which HVAC system should achieve in a vehicle cabin in warm ambient, regarding thermal sensitivity of individual parts of human body obtained from empirical data. Study of passenger thermal sensation and thermal comfort, along with risk of hyperthermia arising due to

high body temperature have been addressed. Human body basics for different subjects (mannequins) and the comfort climate conditions for different subjects have been tested and suggested. Rugh, Chaney and Lustbader [2] suggested on reduction in vehicle temperatures and fuel consumption from cabin ventilation, solar-reflective paint, and a new solar reflective glazing. They were successful in developing a new type of solar reflective glass that improves reflection of the near-infrared (NIR) portion of the solar spectrum. Also solar power car ventilation was tested on Cadillac STS as part of Improved Mobile Air conditioning Cooperative research program (I-MAC). Alexandrov, Kudriavtsev, and Reggio [3] report on use of two and three-dimensional computer simulations to address issues of climate control and performance of HVAC system of a generic passenger car. The paper describes the role of HVAC configuration and design parameters, such as air temperatures and velocities at the inlet, the size, number and location of inlets and outlets. The influence of internal and external parameters on climate conditions inside the car has been discussed in this paper. These results are useful to compare the temperature patterns for the unsteady state thermal analysis.

2. DYNAMIC AIRVENT CONCEPT

Airflow directivity inside a car is mainly influenced by the airduct orientation, number of airvents, shape, and positions of the airvents inside the cabin. All cars come with a standard 4 outlet airvents on the dashboard. Normally, the centre airvents are targeted to cool rear passengers and the side airvents are for driver and co-driver. One of the ways to improve the airflow directivity inside the cabin is by making different shapes of airvents e.g. circular, rectangular, oblong rectangular, squared, a combination of circular and rectangular, etc. In day-to-day life, we use the ceiling fans and table fans. Both the fans have different airflow directivity but serve same purpose i.e. cooling. Human comfort being subjective it is hard to say which one is better. The standard airvent vanes are manually adjusted up/down, right/left by the passengers to direct the airflow. To make these airvent vanes operate automatically a concept called dynamic airvents has been suggested inside the passenger car cabin. These airvents will be coupled with the automatic climate control (ACC) module and will work on stepper motors. Three stepper motors will be used; one for central airvent and two others for side airvents. The input to the motors will be from automatic climate control (ACC) unit. When the cabin temperature rises to a specific level the dynamic vanes will be operational. The motion will continue till 10 minutes with a halt of one minute at the extreme positions. As the temperature drops or maintains the comfort level the HVAC will trip off till the temperature rises again. A periodic movement of the vanes will further reduce the HVAC load and increase fuel efficiency. Air-conditioning with the dynamic airvent feature will rotate the airvent vanes slowly to and fro to distribute the airflow periodically as shown in Figure 1.

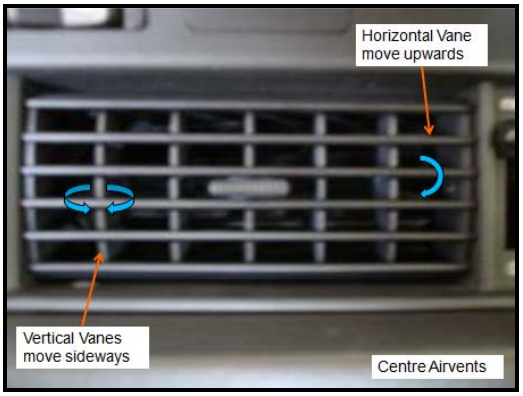

Fig. 1 Dynamic airvent concept

3. SOLUTION PROCEDURE

The airflow of the continuously moving airvent vanes has to be analysed and studied to improve the airflow directivity inside the cabin. The action of moving airvents and the flow directivity can be captured using dynamic meshing in the commercial code FLUENT (ANSYS 13). The dynamic meshing model is used to model flows where the shape of the domain is changing due to motion on the domain boundaries. The motion of the airvent vanes is set by giving the angular velocity about the centre of gravity to each of the vanes. The motion is given through a user defined function (UDF). A UDF is a *C* code including the desired rotation parameters like angular velocity, time etc. The code consists of UDF function called "DEFINE_CG_MOTION" compiled in the FLUENT database (libudf). The update of the volume mesh is handled automatically by FLUENT code at each time step based on the new position of the boundaries. The moving airvent vanes are considered as rigid walls. The initial spacing of the edges before any boundary motion constitutes the equilibrium state of the mesh. The displacement at a given boundary node will generate a force proportional to the displacement along all the springs connected to the node. The force on the mesh node is given by [4, 5]

$$\overrightarrow{Fi} = \sum_{j}^{ni} kij \ (\Delta\overrightarrow{xi} - \Delta\overrightarrow{xj})$$

Where, Δxi and Δxj are displacements of node *i* and neighbouring node *j*,

n_i is the number of connecting neighbouring nodes connected to *i*,

k_{ij} spring stiffness constant.

Boundary node positions are updated from which displacements are known. At convergence the positions are updated such that,

$$xi^{n+1} = xi^{n} + \Delta xi^{m,converged}$$

Where, *n*+1 and *n* are the positions of next and current number of time steps respectively.
The updates of mesh and the wall motion at every time step is shown in Figure 2.

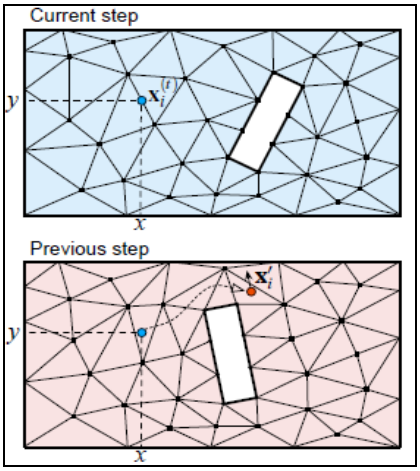

Fig. 2 Representation of wall motion and mesh updates in 2D [5]

Suppose at time *t* velocities are stored at locations *x*(*t*) (the face circumcentres), and to find the velocity at a particular face location *x*(*t*) *i* . It is traced back from *x*(*t*) *i* through the velocity field of the previous time step to a point x_{0i}, which has no necessary correspondence to any feature of the old mesh. Then, the velocity at *x*(*t*) *i* is updated to the value interpolated from the old velocity field at x_{0i}. Because the velocities from the previous step are stored on a different mesh, it has to be traced back and interpolated using this previous mesh. The motion of the vanes is governed by setting the motion attributes. Motion attributes contains parameters to specify the motion attributes for a rigid-body-motion zone and a user-defined-motion zone. The motion of each vane is associated with the centre of gravity location. The C.G. location contains the current values of the coordinates for the location of the C.G. of the respective vane (zone). Further the rotation of the vane is measured under centre of gravity orientation in the FLUENT dynamic meshing card. The total vane rotation from the mean position is measured and stored which is later used to calculate the exact vane angle for respective flow time.

4. GEOMETRIC MODEL

A hatchback passenger car is considered for in-cabin airflow analysis. The geometry of the cabin was prepared using CATIAV5 and imported to HYPERMESH. Water tight geometry with required surfaces has been meshed to capture the surface details. Figure 3 shows the water tight geometry of the cabin. The geometry of the mannequins is separated into three parts namely face, chest and mannequin body to monitor the airflow velocities in detail.

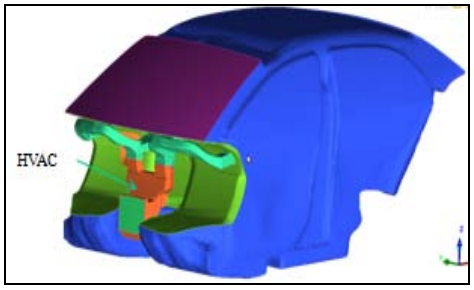

Fig. 3 Geometric Model of Cabin

The HVAC system consists of HVAC inlet, evaporator, closure baffles and HVAC outlet. Blower is not considered for the simplicity of the model. The flow from the HVAC is divided into left and right airducts. The two centre airvents consists of 2 closures, 5 horizontal and 6 vertical vanes. The side airvents consists of 1 closure each, 7 horizontal and 4 vertical vanes. The position of mannequins nose form the airvents is shown in the figure 4.

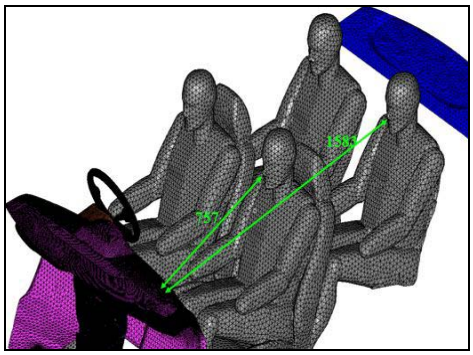

Fig. 4 Mannequins positions from airvents

The water tight geometry is meshed in ICEM-CFD software with prior cleaning of the model as shown in figure 5. The meshed model consists of 12 million tetrahedral cells, with 0.2 skewness quality. A denser mesh has been created just outside the mannequins to capture better airflow characteristics. The airducts have also been meshed denser with mesh size of 3 mm and 1 mm for the vanes. As the dynamic mesh motion is associated with vanes good quality transition inside duct is achieved as shown in the figure 6.

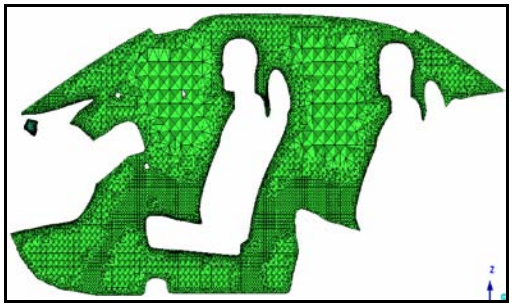

Fig. 5 Meshed section of cabin

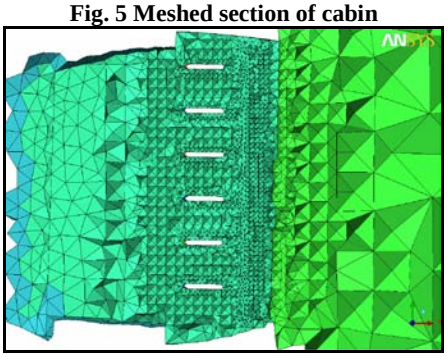

Fig. 6 Cut-section of duct centre vanes

4.1 Calculations

- Mass flow rate: As the blower is not considered for simulation, the mass flow rate is given to HVAC inlet. Flow rate of 0.1426

kg/s (420 CMH) is initialized for the simulation.

- Time step size (Δt): The time step size is the time in seconds for which the simulation progresses. It is calculated from the smallest cell size and initiated velocity and is given as follows,

$$\Delta t \sim \frac{\Delta x}{V}$$

Δx = representative cell size
V = characteristic velocity

The calculated time step size is 0.03 second.

- Number of time steps: The number of time steps for which the flow is to be calculated till the solution reaches convergence. In transient dynamic meshing models time step is of crucial importance and has to be calculated from the moving zones. The extent of the vane was calculated as shown in the figure 7. The vanes are 2 mm thick and hence the cell size of 1 mm is given to capture the geometry. The distance from the extreme position to the duct wall was measured and the final cell size in the duct was decided. This avoids the negative cell volume due to skweness during the mesh motion.

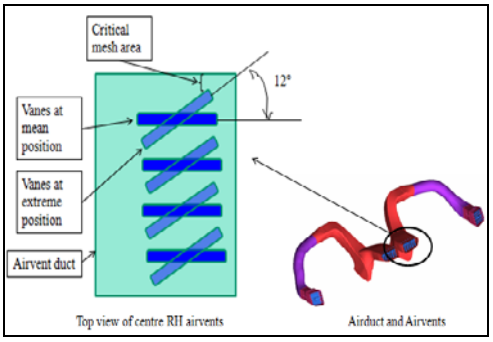

Fig. 7 Plan view of centre right airvents

5. GRID INDEPENDENCE STUDY

As it is difficult to assure that the CFD results for the first run are correct, a grid independence study was done to monitor the results for different grid sizes. Grids consisting of 5, 9, 12 and 15 million tetrahedral cells were used for airflow analysis and the maximum velocities at the mannequin face were compared. The mentioned grids were generated on a 32 core processor and simulations were carried out with 16 GB RAM computing machine. Steady state airflow analysis with first order discretisation scheme for 5 and 12 million mesh models was done and then compared with second order discretisation scheme to check the accuracy in solution. By variation in cabin cell size but keeping the cell size in the rest of the parts same, different grids were created. As higher order schemes give more accurate result, remaining grids were used with second order scheme. Maximum velocities on the face were observed to be no significantly different when the grid was changed from 9-15 million cell models. An adequate grid size of 12 million cells was selected for further transient analysis.

6. RESULTS AND DISCUSSIONS

Airflow directivity analysis for the baseline with steady and dynamic airvents was carried out and compared. For the dynamic airvents, centre vertical vanes were rotated away from each other towards passenger side and stopped at their extreme locations. The analysis was carried out with mass flow inlet of 0.1426 kg/s at the HVAC inlet. Evaporator was considered as porous media with viscous resistance of 2.64×10^9 1/m^2 was calculated from the HVAC characteristics obtained from the vendor. Airflow directivity for the steady case and the case of both vanes moving is compared in the figure 8.

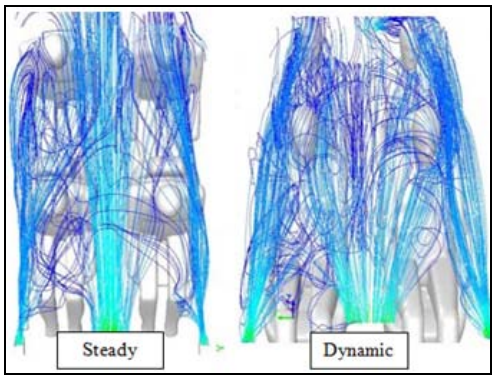

Fig. 8 Pathlines colored with velocity for dynamic and steady airvents model

In steady vanes case the centre vertical vanes are kept at the mean position and the horizontal vanes at their lowest position. As observed the airflow is being directed to the set vane position on the driver and the passenger sides. However, in dynamic vents, the central vertical vanes are rotated by 11 degrees away and horizontal vanes by 7 degrees upwards and stopped. Due to this the flow is being directed in the entire cabin covering maximum parts of the mannequins. Velocity vectors on the nose level plane inside the cabin were plotted as shown in figure 9

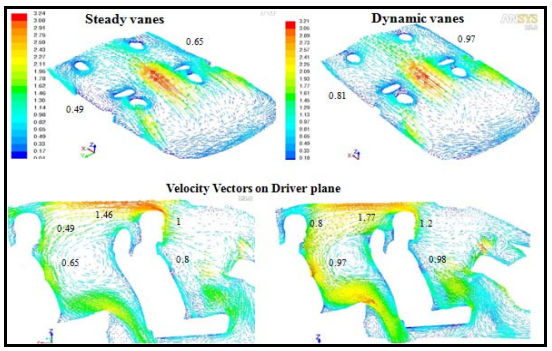

Fig. 9 Velocity vectors for steady and dynamic airvents at nose and driver planes (Z-Z section)

For the steady airvents the flow from the centre airvents are observed to be straight up and then carried away towards the parcel tray. The airflow intensity and velocity appear to be higher at the middle section of the passenger compared to flow at his right and left sides. The flow hits the driver and co-driver seats and a reversed flow is observed due to lack of velocity. The

air velocity decays rapidly just after the front seats as seen in figure 9 (steady, driver-plane). In the dynamic case the rotated vanes direct the flow towards the respective passenger side. A uniform flow pattern is observed hitting the rear passengers. The side airvents direct the flow towards driver and co-driver and also slightly towards rear passengers. Centre airvents cover the entire central path towards the parcel top thereby ensuring total air flow inside the cabin. The driver and co-driver are also being benefited from the centre airvents.

The nose level maximum velocities for the driver and RH passenger are plotted as a function of flow time for the dynamic (both moving) airvents as shown in the figure 10. For the dynamic as the solution advances in time the vertical vanes start moving by 0.34 degrees for each time step of 0.03 seconds. The air velocities start increasing and reach a maximum of 1.2 m/s for driver and 0.8 m/s for the RH Passenger at time equal to 1 second. The recorded vane angle for maximum velocities was 11 degrees for vertical and 7 degrees for horizontal. Both horizontal and vertical vanes stop at respective positions and the flow further continues for 6.5 seconds. For rest of the time flow stabilizes and settles at 1.2 m/s at driver and 0.6 m/s at RH passenger nose level. In the steady state baseline model the flow is observed to stabilize at 0.8 m/s at driver and 0.4 m/s at RH passenger nose level.

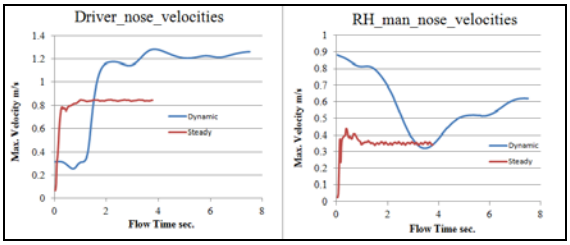

Fig. 10 Comparison of driver and RH passenger nose point velocities with baseline

6.1 Airflow Analysis with Dynamic Airvents, 2 Cycles

To check the airflow for continuously moving vanes case, analysis for 2 cycles of the vanes was carried out. The centre vertical vanes were rotated from their mean position by 11 degrees on either side. Vertical vanes perform two cycles from the mean position as shown in figure 11. The horizontal vanes were moved up by 7 degrees and held there.

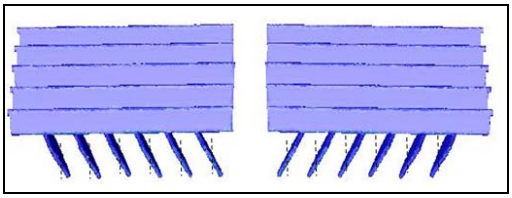

Fig. 11 Vane motion for 2 cycles

As the vertical vanes start moving the flow starts shifting towards the right and left side from the centre. The airflow velocity gradually increases towards the rear side. As the vanes move fast continuously a highly irregular flow pattern is observed which causes turbulence. This process tends to make the flow and the temperature distribution in the cabin more uniform. The airflow is observed to be continuous till the parcel tray. And thus high velocities are recorded for the rear passengers at that time of instance. A wavy pattern of airflow is observed from the centre airvent outlets. This waviness blows air covering upper legs, chest and head. The nose point maximum velocities as the vane moves with time is shown in figure 12. As the vertical vanes reach the first extreme of 11 degrees at 1.8 seconds the maximum velocities for driver and RH passenger recorded are 1.2 m/s and 0.85 m/s respectively. The vanes start moving towards the mean position and arrive at the mean position after around 4 seconds. The respective velocities drop down to a minimum of 0.2 m/s. At this time the entire flow is directed at the middle section of the cabin. The same cycle is repeated for remaining 4 seconds of flow time. In the second cycle the RH passenger receives around 0.7 m/s, slightly less than the first cycle. However this is due to the irregular flow due to the motion of vanes. Thus, a similar pattern will be obtained for further cycles of the vanes.

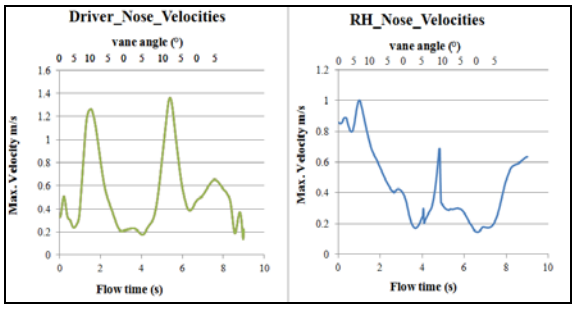

Fig. 12 Nose point velocities, for 2 vane cycles

The airflow directivity on the mannequins is shown in figure 13.

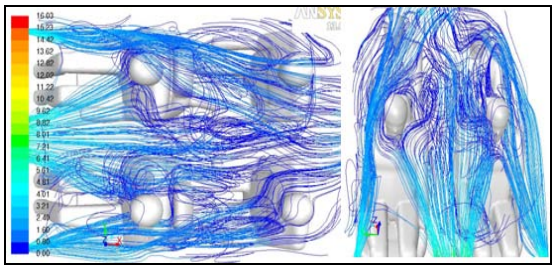

Fig. 13 Airflow directivity with dynamic airvents, 2 cycles

6.2 Comparison of Airflow Velocities for Steady and Dynamic Vents

The nose level velocities for steady and dynamic vents are compared in Table 1. Average air velocity for dynamic vents at the rear passenger was about 0.8 m/s and for the baseline vents 0.53 m/s. Similarly, at the front passenger side it was 1.15 m/s for dynamic and 0.71 m/s for steady case.

	Driver (m/s)	Co-driver	RH Passenger	LH Passenger	Average Velocity

		(m/s)	(m/s)	(m/s)	(m/s)
Baseline (steady airvents)	0.67	0.75	0.5	0.57	0.62
Dynamic Airvents	1.1	1.2	0.75	0.85	0.97

Table 1. Comparison of airflow velocity for steady and dynamic vents

The baseline steady vents show an average velocity of 0.62 m/s. However, with dynamic airvents a rise of 0.27 m/s is observed. Individually the driver and co-driver get ample air flow reaching a maximum of up to 1.2 m/s. The moving airvents also enhances the air flow at rear passenger periodically reaching to maximum of 0.8 m/s.

6.3 Cabin Cool Down Thermal Analysis

As the airflow directivity was examined with dynamic vents, an essential check for its affectivity for cabin cool down is required. Passenger thermal comfort is mainly influenced by the inside cabin temperature. The cabin temperature mainly builds up due to sun's radiation and convection from the windshields, windows and inside cabin components. Plastic components like Instrumental panel, door trims and seatings are also the major sources of heat addition. Cabin cool down test with a convection model has been done to check the effectiveness of dynamic airvents over steady vents. The boundary conditions for the cool down test are listed in Table 2.

Thermal Boundary Conditions	
Temp. at inlet Mass-IN	8° C
Initial Temp. Windows	55° C
Initial Temp. Windshield	67° C
Initial Temp. Cabin	20° C
Initial Temp. Mannequins	37° C

Table 2. Thermal boundary conditions

Steady state thermal analysis was done with steady vanes at mean position. In steady case, the airflow directivity from the central vents is more at the middle zone of the cabin and hence lower temperatures are observed. The rear passengers are exposed to hot air for longer time due to continuous radiation from the windows. Driver and co-driver receive a fair amount of cooling from both the vents. On the other hand, in dynamic vent case the centre vanes move away and lock their positions towards rear passengers. Due to this, rear passengers get better cooling and feel cooler than in the steady vent case. This also enhances cooling at driver and co-driver positions as seen in the plots. The maximum nose level temperatures recorded are 18° C and 20° C for driver and RH passenger respectively. The temperature plots of mannequins for steady and dynamic airvents are shown in figure 14.

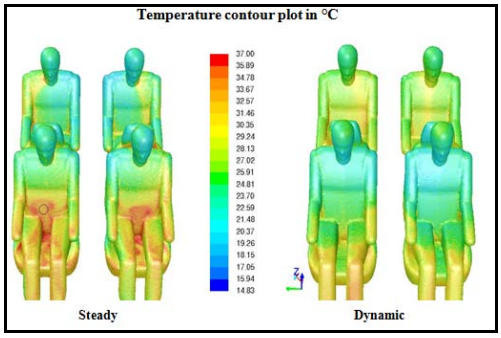

Fig. 14 Temperature contour plots for steady and dynamic vents case

To prevent the rise of body temperature and therefore the risk of hyperthermia, it is necessary to discard heat from the body or to make ambient conditions comfortable by cooling. Largest part of heat loss from the body surface in warm conditions is by convection and by sweat evaporation from the skin. These modes of heat transfer are more intense if difference between skin surface temperature and air temperature is increased and also with an increase of local air velocity. Hence detailed observations for different body surface temperature and the respective velocities are shown in figure 15. The upper body part mainly from waist to head strongly influences thermal sensation.

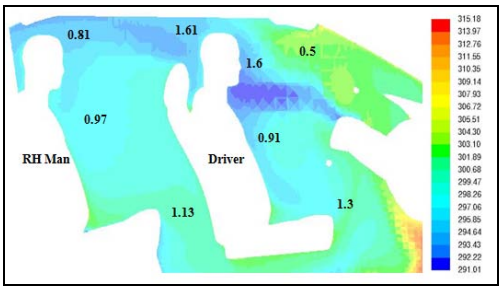

Fig 15. Driver plane temperature contours with air velocities (m/s)

Detailed temperature contour plots at the nose level are obtained and compared as shown in figure 16. The centre part which is the low temperature zone in the steady case is observed to be shifted towards the passenger side in dynamic case, giving better and faster cooling. Low temperature fields are observed at the windows sides compared to steady case. The recorded nose level temperature with the dynamic case for rear the RH and LH passengers are 20° C and 21° C which are lower by 2-3° C than in the baseline case.

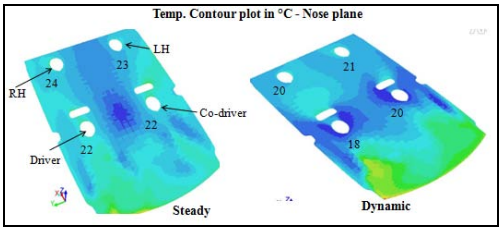

Fig 16. Nose plane temperature plots for steady and dynamic conditions

Usually thermal comfort means that temperature should be between 20° C and 22° C, relative humidity should be about 50% and air velocity should be between 0.5 to 0.8 m/s. To achieve this, a total heat flux that should be transferred out of the car cabin is about 2 kW. The only way to achieve the internal temperature at desired level is to use air conditioning system. An optimum A/C unit should assure thermal comfort under time varying thermal loads with minimal energy consumption. With the dynamic airvents the periodic operation of the vanes will reduce the HVAC load on engine and thereby increase the fuel economy.

7. VALIDATION

The research work done on airflow directivity and thermal analysis was validated with the real time test data. This is required due to the difficulty in modeling the real time boundary conditions. Experimental test results for air flow directivity and cabin cool down have been listed and compared with the simulation.

7.1 Airflow Directivity

The vehicle to be tested was set on idling with full air-conditioning. Pencil type anemometers were mounted at side and centre vent outlets, driver and passenger nose point levels and the respective air velocities were recorded. The air velocities for experimental test and CFD results for baseline steady airvents are compared in the Table 3.

	Driver (m/s)	Co-driver (m/s)	RH Passenger (m/s)	LH Passenger (m/s)	Average Velocity (m/s)
Exptl. test	0.8	0.8	0.6	0.6	0.7
Baseline steady airvents	0.67	0.75	0.5	0.57	0.62

Table 3. Validation of air velocities for baseline with test results

The CFD analysis was carried out with a mass flow rate of 0.1426 kg/s. However, the actual test was done considering the blower. The baseline air flow velocities are observed to be close to the actual test data.

7.2 Cabin Cool Down Test

The cabin cool down test was carried out to check the cooling effect of air-conditioning with different vent angles. The test was carried for 90 minutes, with 60 minutes solar load and 30 minutes cool down with full air-conditioning at mean vane position.

	Driver (°C)	Co-driver (°C)	RH Passenger (°C)	LH Passenger (°C)	Avg. nose temp (°C)
Exptl. Test	19	19	20	20	19.5
Baseline Steady airvents (CFD)	22	22	23	24	22.75

Table 4. Validation of nose level temperature for baseline with test results

The test was carried out at 35° C ambient temperature. Thermocouples were mounted at vent outlets and mannequins nose positions to measure the temperature. The recorded average nose temperature for the experimental test and simulation are listed in the Table 4. The cabin temperature builds up to 65° C during soaking, and starts dropping down to a minimum of 19.5° C during the cool down cycle. The average cabin temperature settles to around 20º C for the rest of the time. However in the baseline the average temperature settles at 22º C due to lack of airflow at the rear side. A difference of 2° C is observed which may be due to the convection model considered for the simulation. The cabin temperature form the start of the cool down cycle is monitored at the respective mannequins nose levels. Temperature plot as a function of flow time for the dynamic airvent simulation has been compared with the experimental test data as shown in the figure 17. The comparison is made to monitor the temperature values with the benchmarked temperature values. Both temperature curves show similar trend. A slightly faster cool down in seen with the dynamic airvents compared to experimental test results. However in both the cases the cabin temperature settles down to 20º C.

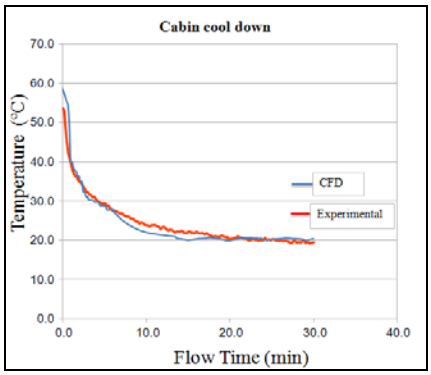

Fig. 17 Cabin cool down temperatures

The comparison for the airflow and cabin cool down for baseline shows that the results are within the benchmarked values. Also the simulation results for the dynamic airvents show almost same trend as of experimental test. Hence, these results can be further used for different dynamic cycles and can be compared.

8. CONCLUSIONS

In the present study, dynamic airvents concept has been proposed to improve thermal comfort for passengers and improve HVAC efficiency. We found that airflow directivity is improved for the rear passengers due to moving of the airvent vanes from the mean position. The dynamic vanes have enhanced the air flow for driver & co-driver and throughout the cabin. Airflow throughout the cabin has helped in reducing the overall cabin temp. by about 3°C. The cabin cool down rate is faster by dynamic airvents compared to the steady airvents (baseline) and the temperature settles to steady 20° C.

9. REFERENCES

[1] Ruzic, D. (2011) *"Improvement of Thermal Comfort in a Passenger Car by localized air distribution"*, Acta Technical Corviniesis-Bulletin of Engineering, ISSN 2067-3809.

[2] Rugh, J.P., Chaney, L. and Lustbader, J. (2007) *"Reduction in Vehicle Temperatures and Fuel Use from Cabin Ventilation, Solar-Reflective Paint,*

and a New Solar-Reflective Glazing", SAE World Congress, 16-19.

[3] Alexandrov, A., Kudriavtsev, V., and Reggio, M. (2001) "*Analysis of Flow Patterns and Heat Transfer in Generic Passenger Car Mini-Environment"*, 9th Annual Conference of CFD Society of Canada, Kitchener, Ontario, 27-29.

[4] Klinger, B.M., Feldman, B.M., and Brein, J. (2006) *"Fluid Animation with Dynamic Meshes"*, Computer Graphics Proceedings, Annual Conference Series.

[5] Kelecy, F. (2005) "*Modeling Transient flows with FLUENT 6*", FLUENT Inc.